Proceedings of the ASME 2016 International Design Engineering Technical Conferences & Computers and Information in Engineering Conference
IDETC/CIE 2016
August 21-24, 2016, Charlotte, NC, USA

DETC2016-59291

SPATIAL 3-SUR 1-RU PLATFORM ROBOT INVERSE ORIENTATION KINEMATICS

Robert L. Williams II, Ph.D.
Mechanical Engineering Department
Ohio University
Athens, Ohio, USA
williar4@ohio.edu

Elvedin Kljuno, Ph.D.
Mechanical Engineering Department
University of Sarajevo
Sarajevo, Bosnia
rl133112@ohio.edu

J. Jim Zhu, Ph.D.
Electrical Engineering
Ohio University
Athens, Ohio, USA
zhuj@ohio.edu

ABSTRACT

This paper describes the spatial three-dof 3-SUR 1-RU spherical Parallel Platform Robot. This type of robot has been previously proposed by other authors, but the present design, platform-mounted actuators, and application are unique. Further, the inverse kinematics problem is solved analytically. This robot is under development at Ohio University to serve as the active orienting device for aerodynamic testing of unmanned aerial vehicles (UAV) with up to 3 m wingspan. The UAV will be tested on a Windmobile which is a ground vehicle that is driven with the test article on an instrumented truss extended in the front in an undisturbed flow field. This system is an inexpensive substitute for a large-scale wind tunnel for measuring aerodynamic parameters of the UAV.

The three-degrees-of-freedom (dof) of the platform robot are actively controlled by three servomotors (R joints) mounted to the underside of the moving platform and there is a passive fourth middle leg with passive R-U joints for support. The inverse orientation kinematics (IOK) problem is formulated and solved analytically in this paper. Given the three desired Euler Angles, the three required actuator angles are found. Geometrically this analytical solution is equivalent to finding the intersection point of two circles on different planes, independently for each of the three platform robot legs. The analytical solution requires finding the roots of a quartic polynomial. There are at most two real solutions (elbow-up and elbow-down) which means that there are always at least two imaginary solutions to the IOK problem, which are discarded. Examples are presented to demonstrate the platform robot IOK solution algorithm for use in practical platform robot control.

KEYWORDS

Windmobile, Galah UAV, Spatial parallel platform robot, inverse orientation kinematics, analytical solution algorithm, multiple solutions, algorithmic singularity, imaginary solutions.

1. INTRODUCTION

Parallel manipulators are known as mechanical systems that generally have a base and a platform, which are connected together by computer controlled serial kinematic chains. The kinematic chains, referred to as the legs, work together to control a single platform or end-effector. Parallel manipulators are known to have some advantages over their serial counterparts such as higher rigidity, higher load capacity, and better positioning accuracy [1]. There are many types of parallel manipulator systems; a well-known parallel manipulator is the Stewart Platform, typically comprised of six linear actuators guiding the moving platform. This parallel manipulator is used in applications such as flight and automotive simulation. One study examined the use of such a system to evaluate biomechanical functions such as joint laxity [2].

There are many difficulties that arise in studying parallel robotic manipulators. These problems include complex kinematic and dynamic equations. It is generally found in parallel robotic kinematic analysis that the inverse kinematic solution is easier to obtain than the forward kinematics solution. The forward kinematics solution is difficult due to the

fact that it requires the solution of multiple coupled nonlinear (transcendental) algebraic equations from the vector loop-closure equations. This in turn leads to multiple valid solutions for the forward kinematics problem. Another difficulty that arises is the complex control of the kinematic chains. It is important to make sure that the linear actuators are programmed to work in conjunction with each other to provide the right motion for the platform. When looking at parallel robotic manipulator systems, it can be observed that there would be a problem with the configuration space, as the system has a limited workspace due to the constraining legs. The problem with this is that the configuration space is never explicitly known. Another difficulty is that singularities are found in the end-effector, the configuration space, and the actuators of the system [3].

Only three degrees of freedom (dof) are needed in many parallel robot applications [4]. In the current paper, only spatial orientations are required for the Windmobile system, so our robot has only three-dof. Our literature review revealed no robot that we propose, but three similar ones.

Di Gregorio [4] presented a 3-UPU parallel manipulator for three-dof wrist applications, composed of a base and end effector connected by three UPU legs (the underbar indicates that it is the prismatic joint being actuated in each leg). Zeng et al. [1] studied a 3-PRUR parallel manipulator. In this manipulator there are three translational dof. The workspace of a parallel manipulator depends on the mechanical limits and interferences amongst the legs of the manipulator, extreme displacements of the actuators, and singularity constraints [1]. Deidda et al. [5] presented a 3-RRUR spherical parallel manipulator. This robot makes use of equivalent planar joints as opposed to equivalent spherical joints to simplify assembling issues. The applications of this robot include an orientation wrist for cameras, medical devices, haptic interfaces, and sensors [5].

The proposed parallel robot in this manuscript is similar to classical 3-dof spherical parallel robots [6], but the actuation scheme is novel and a passive RU middle leg has been added.

The current paper first presents a brief overview of our UAV Windmobile Project, followed by a description of the designed 3-SUR 1-RU parallel platform robot, the analytical solution of the crucial inverse orientation kinematics problem, followed by snapshot examples to demonstrate this solution.

2. WINDMOBILE PROJECT INFORMATION

This paper introduces a new three-dof 3-SUR 1-RU parallel platform robot designed for orienting a UAV. The Windmobile being developed at Ohio University will first be used to obtain basic aerodynamic coefficients of the Galah UAV (Figure 1) at different angles of attack and sideslip angles.

The designed Windmobile consists of a van mounted with a truss system (Figure 2). The truss system is attached to the front of the van such that the test article is extended into a relatively-undisturbed flow field. In place of the Load cell sting / vibration isolator shown in Figure 2, we plan to mount the 3-SUR 1-RU robot for orienting the UAV during van/runway experiments to gather flight characteristics. This method will prove to be considerably cheaper and more accessible (albeit less accurate) than testing UAV characteristics with a conventional wind tunnel. However, the accuracy should be adequate for an initial design of the autopilot controller gains to facilitate effective and safe tuning of the autopilot.

The Windmobile Project needs a system that can attach the aircraft to the truss system, so as to be able to control the UAV's yaw, pitch, and roll orientation angles in order to set and regulate the aerodynamic angles in the presence of environmental disturbances and road surface irregularities. We propose our new 3-SUR 1-RU parallel platform robot for this purpose. The currently-proposed robot is similar to existing 3-dof spherical parallel robots, though with different actuation, passive middle leg, and design. The parallel robotic system will be connected to the fuselage of the UAV. The 3-SUR 1-RU system will then be able to manipulate the UAV yaw, pitch, and roll by adjusting the legs of the manipulator. The system will use three moving-platform-mounted servomotors that will provide the three-dof actuation.

Figure 1. Galah UAV

Figure 2. Windmobile Conceptual Design

3. 3-SUR 1-RU PLATFORM ROBOT

This section describes the three-dof 3-SUR 1-RU Parallel Platform Robot. Figure 3 shows a CAD model of this robot and Figure 4 shows the kinematic diagram. For clarity, Figure 4 is shown upside-down compared to the real-world orientation of Figures 3. As seen in Figure 4, the base Cartesian reference frame is {0}, attached in the center of the base platform, with coordinate axes directions as shown. The moving platform Cartesian reference frame is {*P*}, attached to the center of the moving platform, with coordinate axes directions as shown. The three-dof are actively controlled by three rotational servomotors, mounted to the underside of the moving platform.

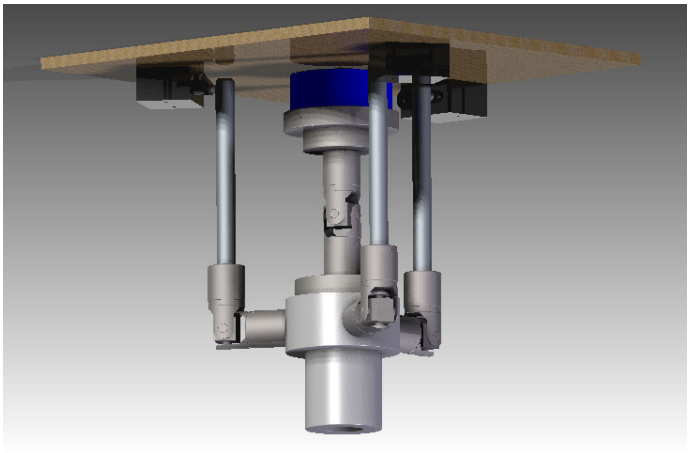

Figure 3a. Three-dof 3-SUR 1-RU Parallel Platform Robot CAD Model

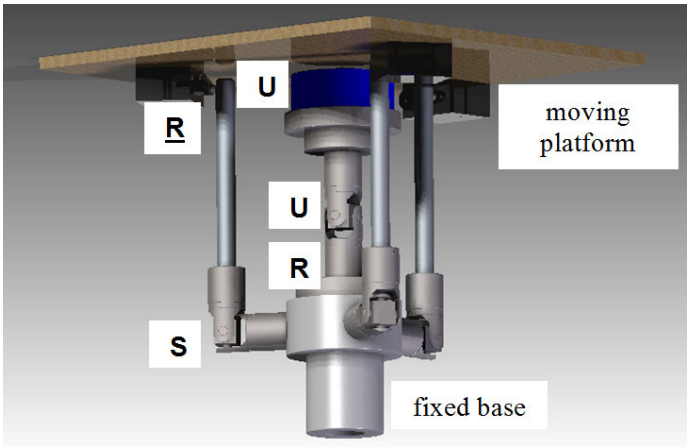

Figure 3b. Three-dof 3-SUR 1-RU Parallel Platform Robot CAD Model Annotated

The passive R-U leg is included in the middle to bear a significant portion of the weight and dynamic loads of the moving platform with mounted aircraft.

The robot is composed of three Spherical-Universal-Revolute (SUR) jointed legs in parallel, connecting the base to the moving platform. The underbar on the revolute joint indicates that it is the actuated joint in each case, while the S and U joints are passive. A different, passive, RU fourth leg connecting the base to the moving platform exists in the middle, to bear the primary load. That R joint rotates relative to the base, and the U joint rotates relative to the moving platform. A small rigid link connects the middle RU joints.

In this design there are $N = 9$ links, $J_1 = 4$ one-dof R joints, $J_2 = 4$ two-dof U joints, and $J_3 = 3$ three-dof S joints. Therefore, the spatial Kutzbach mobility equation yields three-dof, as required:

$$M = 6(N-1) - 5J_1 - 4J_2 - 3J_3 - 2J_4 - 1J_5$$
$$M = 6(9-1) - 5(4) - 4(4) - 3(3)$$
$$M = 3 \quad \text{dof}$$

This mobility result means that the three moving-platform-mounted motors (the three active R joints) are sufficient to control the moving platform orientation in general 3D rotations.

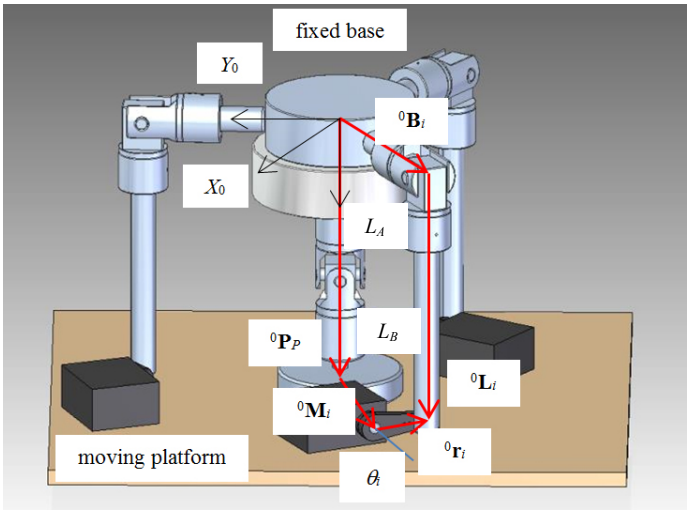

Figure 4. Three-dof 3-SUR 1-RU Parallel Platform Robot Kinematic Diagram (upside-down)

As shown in the kinematic diagram of Figure 4, lengths L_A and L_B are the link lengths connected to the base and moving platforms, at the origins of {0} and {*P*}, respectively, connected at the center of the central U joint.

Figure 5 shows kinematic details for the fixed base platform and Figure 6 shows kinematic details for the moving platform. As seen in Figure 5, the fixed platform base S joint points B_i are located by known constant polar coordinates (R_i, δ_i), $i = 1,2,3$, with respect to base frame {0}. As shown in Figure 6, the moving platform motor points M_i are located by known constant offset polar coordinates $(P_i, \varepsilon_i, r_i)$, $i = 1,2,3$ equivalent, with respect to moving frame {*P*}.

The absolute fixed base point vectors B_i (see Figure 5) are calculated as follows, with respect to {0} coordinates.

$$\left\{ {}^0\mathbf{B}_i \right\} = \begin{Bmatrix} B_{ix} \\ B_{iy} \\ B_{iz} \end{Bmatrix} = \begin{Bmatrix} R_i \cos\delta_i \\ R_i \sin\delta_i \\ 0 \end{Bmatrix} \tag{1}$$

The relative moving platform point vectors M_i (see Figure 6) are constant with respect to moving platform $\{P\}$ coordinates, and calculated as follows (each M_i point is set corresponding to $\theta_i = 0$) .

$$\left\{ {}^{P}\mathbf{M}_i \right\} = \begin{Bmatrix} M_{ix} \\ M_{iy} \\ M_{iz} \end{Bmatrix} = \begin{Bmatrix} P_i \cos\varepsilon_i - r_i \sin\varepsilon_i \\ P_i \sin\varepsilon_i + r_i \cos\varepsilon_i \\ 0 \end{Bmatrix} \qquad (2)$$

Each of the three SUR legs, $i = 1,2,3$, is constructed in a similar manner to the others. A rigid link of length L_i connects fixed spherical joint point B_i to the moving U joint. A rigid link of length r_i connects the moving, active revolute joint point M_i to the same moving U joint. The active revolute joint variable is θ_i.

The equations in this document are derived in general, for the general 3-SUR 1-RU parallel platform robot. The perfect symmetry case could lead to significant simplifications in the equations, and is expressed by the following.

$$\begin{aligned} R_1 &= R_2 = R_3 = R & r_1 &= r_2 = r_3 = r \\ L_1 &= L_2 = L_3 = L & \delta_1 &= \varepsilon_1 = 330^\circ \\ L_A &= L_B = \frac{L}{2} & \delta_2 &= \varepsilon_2 = 90^\circ \\ P_1 &= P_2 = P_3 = P = R & \delta_3 &= \varepsilon_3 = 210^\circ \end{aligned} \qquad (3)$$

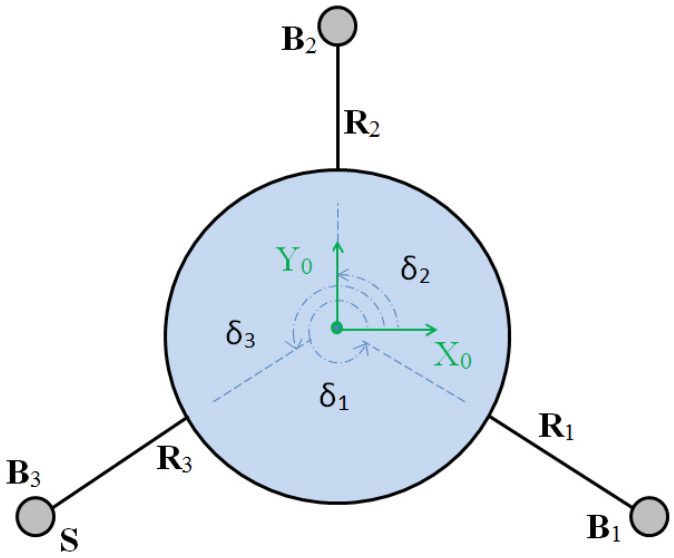

Figure 5. Fixed Base Platform Kinematic Details

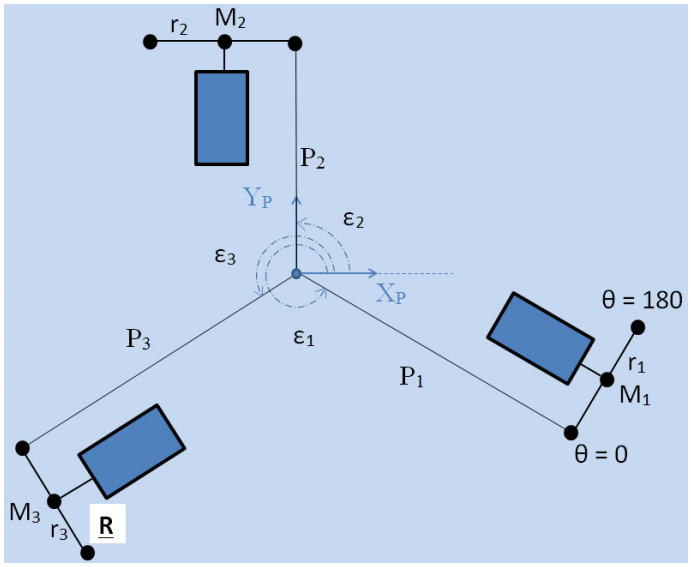

Figure 6. Moving Platform Kinematic Details

4. 3-SUR 1-RU KINEMATICS ANALYSIS

From the kinematic diagram of Figure 4, three vector loop-closure equations are written to form the basis of kinematic analysis. All vectors must be written in the same frame; {0} is chosen as the frame of coordinate expression here.

$$\left\{ {}^{0}\mathbf{P}_P \right\} + \left\{ {}^{0}\mathbf{M}_i \right\} + \left\{ {}^{0}\mathbf{r}_i \right\} = \left\{ {}^{0}\mathbf{B}_i \right\} + \left\{ {}^{0}\mathbf{L}_i \right\} \qquad i = 1,2,3 \qquad (4)$$

The second and third vectors of equations (4) are more conveniently expressed initially in the moving platform frame $\{P\}$, leading to the following expression of the three vector loop-closure equations. The vectors $\left\{ {}^{P}\mathbf{M}_i \right\}$ and $\left\{ {}^{0}\mathbf{B}_i \right\}$ were presented previously. All vectors are defined in the table below.

$$\left\{ {}^{0}\mathbf{P}_P \right\} + \left[{}^{0}_{P}\mathbf{R} \right] \left\{ {}^{P}\mathbf{M}_i \right\} + \left[{}^{0}_{P}\mathbf{R} \right] \left\{ {}^{P}\mathbf{r}_i \right\} = \left\{ {}^{0}\mathbf{B}_i \right\} + \left\{ {}^{0}\mathbf{L}_i \right\}$$
$$i = 1,2,3 \qquad (5)$$

$\left\{ {}^{0}\mathbf{P}_P \right\}$	absolute position vector from origin {0} to origin {P}, expressed in {0} coordinates
$\left\{ {}^{P}\mathbf{M}_i \right\}$	relative position vector from origin {P} to motor point {M_i}, expressed in {P} coordinates
$\left\{ {}^{0}\mathbf{M}_i \right\}$	relative position vector from origin {P} to motor point {M_i}, expressed in {0} coordinates
$\left\{ {}^{P}\mathbf{r}_i \right\}$	relative position vector from motor point {M_i} to U-joint i, expressed in {P} coordinates
$\left\{ {}^{0}\mathbf{r}_i \right\}$	relative position vector from motor point {M_i} to U-joint i, expressed in {0} coordinates
$\left\{ {}^{0}\mathbf{B}_i \right\}$	absolute position vector from origin {0} to based-mounted S-joint i (point B_i), expressed in {0} coordinates
$\left\{ {}^{0}\mathbf{L}_i \right\}$	relative position vector from based-mounted S-joint i (point B_i) to U-joint i, expressed in {0} coordinates
$\left[{}^{0}_{P}\mathbf{R} \right]$	orthonormal rotation matrix giving the orientation of {P} with respect to {0}

Now the remaining terms for equations (5) are presented. Adopting the *Z-Y-X* (α–β–γ) Euler angles convention [7], the

orthonormal rotation matrix $\left[{}^{0}_{P}\mathbf{R}\right]$ giving the orientation of the moving platform frame $\{P\}$ with respect to the fixed base frame $\{0\}$ is:

$$\left[{}^{0}_{P}\mathbf{R}\right]=\begin{bmatrix} r_{11} & r_{12} & r_{13} \\ r_{21} & r_{22} & r_{23} \\ r_{31} & r_{32} & r_{33} \end{bmatrix} = \begin{bmatrix} c\alpha c\beta & -s\alpha c\gamma + c\alpha s\beta s\gamma & s\alpha s\gamma + c\alpha s\beta c\gamma \\ s\alpha c\beta & c\alpha c\gamma + s\alpha s\beta s\gamma & -c\alpha s\gamma + s\alpha s\beta c\gamma \\ -s\beta & c\beta s\gamma & c\beta c\gamma \end{bmatrix} \tag{6}$$

Throughout this paper *c* will commonly be used as the abbreviation of *cosine* and *s* will commonly be used as the abbreviation of *sine*, for various angles.

From a vector loop-closure equation of the central, different leg of the robot with the passive R-U joint, $\left\{{}^{0}\mathbf{P}_{P}\right\}$ is calculated.

$$\begin{aligned} \left\{{}^{0}\mathbf{P}_{P}\right\} &= \left\{{}^{0}\mathbf{L}_{A}\right\}+\left\{{}^{0}\mathbf{L}_{B}\right\} = \begin{Bmatrix} 0 \\ 0 \\ L_A \end{Bmatrix} + \left[{}^{0}_{P}\mathbf{R}\right]\begin{Bmatrix} 0 \\ 0 \\ L_B \end{Bmatrix} \\ &= \begin{Bmatrix} 0 \\ 0 \\ L_A \end{Bmatrix} + \begin{Bmatrix} (\ s\alpha s\gamma + c\alpha s\beta c\gamma)L_B \\ (-c\alpha s\gamma + s\alpha s\beta c\gamma)L_B \\ c\beta c\gamma L_B \end{Bmatrix} = \begin{Bmatrix} r_{13}L_B \\ r_{23}L_B \\ r_{33}L_B + L_A \end{Bmatrix} \end{aligned} \tag{7}$$

Vector $\left\{{}^{0}\mathbf{L}_{i}\right\}$ is simply expressed as three *XYZ* components for each of the outer legs.

$$\left\{{}^{0}\mathbf{L}_{i}\right\}=\begin{Bmatrix} L_{ix} \\ L_{iy} \\ L_{iz} \end{Bmatrix} \qquad i=1,2,3 \tag{8}$$

With the aid of Figures 7, vector $\left\{{}^{P}\mathbf{r}_{i}\right\}$ can be derived, where ε_i are the three fixed and given platform angles (see Figure 6), and θ_i are the three variable and active joint angles, controlled by the servomotors.

$$\left\{{}^{P}\mathbf{r}_{i}\right\}=\begin{Bmatrix} r_i\cos\theta_i\cos\left(\varepsilon_i-\dfrac{\pi}{2}\right) \\ r_i\cos\theta_i\sin\left(\varepsilon_i-\dfrac{\pi}{2}\right) \\ -r_i\sin\theta_i \end{Bmatrix} = \begin{Bmatrix} r_i\cos\theta_i\sin\varepsilon_i \\ -r_i\cos\theta_i\cos\varepsilon_i \\ -r_i\sin\theta_i \end{Bmatrix} \qquad i=1,2,3 \tag{9}$$

Isolating $\left\{{}^{0}\mathbf{L}_{i}\right\}$ and substituting all of the appropriate parameters and derived terms into the vector loop-closure equations (5) yields:

$$\left\{{}^{0}\mathbf{L}_{i}\right\}=\left\{{}^{0}\mathbf{P}_{P}\right\}+\left[{}^{0}_{P}\mathbf{R}\right]\left\{{}^{P}\mathbf{M}_{i}\right\}+\left[{}^{0}_{P}\mathbf{R}\right]\left\{{}^{P}\mathbf{r}_{i}\right\}-\left\{{}^{0}\mathbf{B}_{i}\right\}$$

$$\begin{Bmatrix} L_{ix} \\ L_{iy} \\ L_{iz} \end{Bmatrix} = \begin{Bmatrix} r_{13}L_B \\ r_{23}L_B \\ r_{33}L_B + L_A \end{Bmatrix} + \begin{bmatrix} r_{11} & r_{12} & r_{13} \\ r_{21} & r_{22} & r_{23} \\ r_{31} & r_{32} & r_{33} \end{bmatrix}\begin{Bmatrix} M_{ix} \\ M_{iy} \\ 0 \end{Bmatrix} + \begin{bmatrix} r_{11} & r_{12} & r_{13} \\ r_{21} & r_{22} & r_{23} \\ r_{31} & r_{32} & r_{33} \end{bmatrix}\begin{Bmatrix} r_i\,\mathrm{c}\,\theta_i\,\mathrm{s}\,\varepsilon_i \\ -r_i\,\mathrm{c}\,\theta_i\,\mathrm{c}\,\varepsilon_i \\ -r_i\,\mathrm{s}\,\theta_i \end{Bmatrix} - \begin{Bmatrix} B_{ix} \\ B_{iy} \\ 0 \end{Bmatrix}$$

$$i=1,2,3 \tag{10}$$

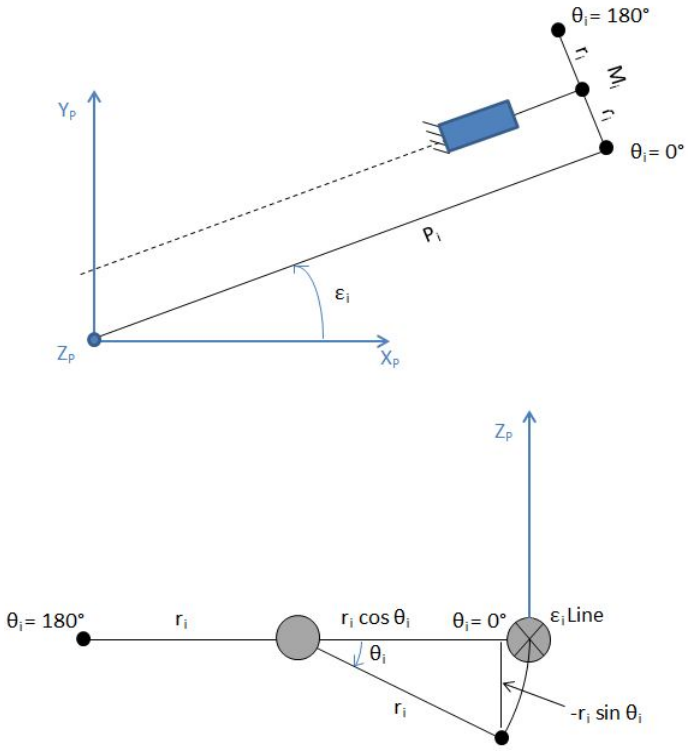

Figure 7. $\left\{{}^{P}\mathbf{r}_{i}\right\}$ Kinematic Details

The vector loop-closure equation yields three scalar equations for each of the three in-parallel legs. Many terms are shared amongst all nine scalar equations, notably the Euler angles α, β, γ included in the r_{ij} terms of (10), defined from (6).

$$\begin{aligned} L_{ix} &= r_{13}L_B + r_{11}M_{ix} + r_{12}M_{iy} + r_{11}r_i\,\mathrm{c}\,\theta_i\,\mathrm{s}\,\varepsilon_i - r_{12}r_i\,\mathrm{c}\,\theta_i\,\mathrm{c}\,\varepsilon_i - r_{13}r_i\,\mathrm{s}\,\theta_i - B_{ix} \\ L_{iy} &= r_{23}L_B + r_{21}M_{ix} + r_{22}M_{iy} + r_{21}r_i\,\mathrm{c}\,\theta_i\,\mathrm{s}\,\varepsilon_i - r_{22}r_i\,\mathrm{c}\,\theta_i\,\mathrm{c}\,\varepsilon_i - r_{23}r_i\,\mathrm{s}\,\theta_i - B_{iy} \\ L_{iz} &= r_{33}L_B + L_A + r_{31}M_{ix} + r_{32}M_{iy} + r_{31}r_i\,\mathrm{c}\,\theta_i\,\mathrm{s}\,\varepsilon_i - r_{32}r_i\,\mathrm{c}\,\theta_i\,\mathrm{c}\,\varepsilon_i - r_{33}r_i\,\mathrm{s}\,\theta_i \end{aligned}$$

$$i=1,2,3 \tag{11}$$

The kinematics equations come from the constraint that each rigid link vector $\left\{{}^{0}\mathbf{L}_{i}\right\}$, $i=1,2,3$, must have known constant length L_i:

$$L_i=\left\|\left\{{}^{0}\mathbf{L}_{i}\right\}\right\|=\sqrt{L_{ix}^2+L_{iy}^2+L_{iz}^2} \qquad i=1,2,3 \tag{12}$$

where the Euclidean norm is used in (12).

In general (12) represents three hyper-complicated equations relating the three active joint variables $\{\boldsymbol{\Theta}\} = \{\theta_1 \quad \theta_2 \quad \theta_3\}^T$ to the three Cartesian orientation variables (Euler angles) α, β, γ, represented in the r_{ij} terms, given in (6). A simplification is obtained by squaring both sides of (12):

$$L_i^2 = L_{ix}^2 + L_{iy}^2 + L_{iz}^2 \qquad i = 1,2,3 \quad (13)$$

5. 3-SUR 1-RU INVERSE ORIENTATION KINEMATICS SOLUTION

The inverse orientation kinematics (IOK) problem is stated: Given the desired platform Cartesian orientation $\left[{}^0_P\mathbf{R}\right]$ specified by the Euler angles α, β, γ, calculate the three active servomotor angles $\{\boldsymbol{\Theta}\} = \{\theta_1 \quad \theta_2 \quad \theta_3\}^T$. This IOK solution is useful in controls since the user or computer specifies what the platform orientation trajectory should be and the inverse orientation kinematics solution calculates the three servomotor angles at each time instant to achieve these commanded orientations.

Analytical Solution

The IOK solution is derived analytically as follows. The same steps apply to all three outer legs independently – we will now drop the i notation for clarity. The hyper-complicated equations (14) turn out to simplify amazingly when all details (chiefly α, β, γ) are substituted. Using the MATLAB Symbolic Math Toolbox yielded the following equation to solve:

$$E\cos\theta + F\sin\theta + G = 0 \qquad (14)$$

where:

$$E = 2r[L_A(r_{31}s\varepsilon - r_{32}c\varepsilon) - B_x(r_{11}s\varepsilon - r_{12}c\varepsilon) - B_y(r_{21}s\varepsilon - r_{22}c\varepsilon) + M_x s\varepsilon - M_y c\varepsilon]$$

$$F = 2r[-L_A r_{33} - L_B + B_x r_{13} + B_y r_{23}]$$

$$G = B_x^2 + B_y^2 + L_A^2 + L_B^2 + M_x^2 + M_y^2 + r^2 - L^2 + 2[L_A(M_x r_{31} + M_y r_{32} + L_B r_{33}) - L_B(B_x r_{13} + B_y r_{23}) - B_x(M_x r_{11} + M_y r_{12}) - B_y(M_x r_{21} + M_y r_{22})]$$

This well-known equation form (14) is identical to an equation from standard four-bar mechanism position analysis; hence we expect two valid solutions for each θ. The E, F, G terms are quite different from the four-bar mechanism case, of course, but are calculated in the current problem from all known terms (given constants and the required orientation variables α, β, γ are given at each time snapshot, calculating all r_{ij} terms).

There are a few existing methods for solution of Equation (14). Using the tangent half-angle substitution approach:

$$t = \tan\left(\frac{\theta}{2}\right) \qquad \cos\theta = \frac{1-t^2}{1+t^2} \qquad \sin\theta = \frac{2t}{1+t^2}$$

the solution for θ is:

$$t_{1,2} = \frac{-F \pm \sqrt{E^2 + F^2 - G^2}}{G - E} \qquad (15)$$

$$\theta_{1,2} = 2\tan^{-1}(t_{1,2}) \qquad (16)$$

There are two possible solutions 1,2 for each of the three legs $i = 1,2,3$, in each case corresponding to elbow up and elbow down. Therefore, for the overall 3-SUR 1-RU robot IOK solution, there are a total of $2^3 = 8$ possible solutions.

This concludes the analytical IOK solution for the 3-SUR 1-RU platform robot. It is applied independently to each of the three outer legs. Now we present an alternate analytical IOK solution based on geometry, again applied independently leg-by-leg.

Alternate Geometric Solution

Geometrically the IOK solution for each leg requires the intersection of a known sphere with a known circle, yielding two possible solutions (elbow up and elbow down for each outer leg). The known sphere has radius L_i whose center is base point B_i. The known circle has radius r_i from known center M_i (derived from the given α, β, γ).

For convenience in this solution for each outer leg, choose a local coordinate frame fixed in the plane of the known circle, whose origin is moving platform motor point M_i. In this coordinate frame, using transformations, calculate the vector to the center of the sphere and let these XYZ coordinates be (a,b,c), as shown in Figure 8.

The required vector-loop-closure equation and transformations to calculate the XYZ coordinates (a,b,c) are given below. Again, (a,b,c) gives the center of the sphere of radius L_i from the center of the motor rotation, in the local motor coordinates shown in Figure 8.

$$\left\{{}^{M_i}\mathbf{P}_{B_i}\right\} = \begin{Bmatrix} a \\ b \\ c \end{Bmatrix} = \left[{}^{M_i}_0\mathbf{R}\right]\left\{{}^0\mathbf{P}_{B_i} - {}^0\mathbf{P}_{M_i}\right\} \qquad (17)$$

where:

$$\left\{{}^0\mathbf{P}_{M_i}\right\} = \left\{{}^0\mathbf{P}_P\right\} + \left[{}^0_P\mathbf{R}\right]\left\{{}^P\mathbf{P}_{M_i}\right\} \qquad (18)$$

$$\left[{}^{M_i}_{0}\mathbf{R} \right] = \left[{}^{M_i}_{P}\mathbf{R} \right] \left[{}^{P}_{0}\mathbf{R} \right] \tag{19}$$

Where the three $\left[{}^{M_i}_{P}\mathbf{R} \right] = \left[{}^{P}_{M_i}\mathbf{R} \right]^{-1} = \left[{}^{P}_{M_i}\mathbf{R} \right]^{T}$ orthonormal rotation matrices, $i = 1,2,3$, are found from simple rotations about Z_P by angle ε_i (see Figure 7 top):

$$\left[{}^{P}_{M_i}\mathbf{R} \right] = \begin{bmatrix} \cos\varepsilon_i & -\sin\varepsilon_i & 0 \\ \sin\varepsilon_i & \cos\varepsilon_i & 0 \\ 0 & 0 & 1 \end{bmatrix} \tag{20}$$

and $\left[{}^{P}_{0}\mathbf{R} \right] = \left[{}^{0}_{P}\mathbf{R} \right]^{-1} = \left[{}^{0}_{P}\mathbf{R} \right]^{T}$.

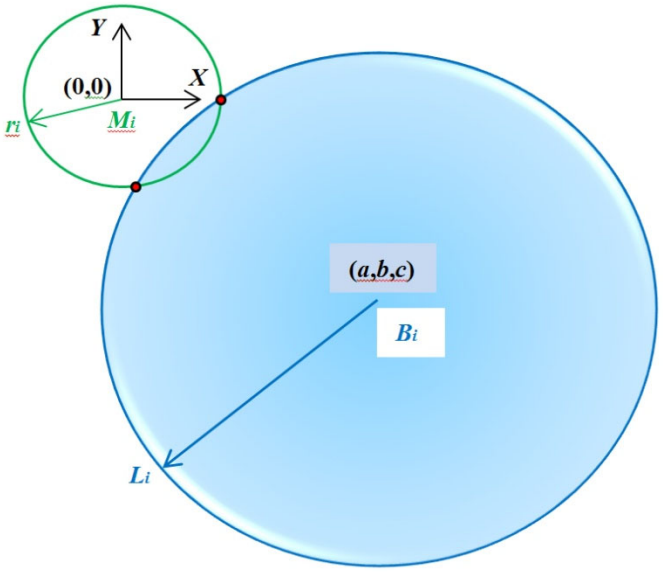

Figure 8. Circle / Sphere Intersections

The solution for the two possible intersection points between a known circle and sphere with the coordinates and notation of Figure 8 is now derived. With reference to the coordinate frame of Figure 8, the equations for the known circle and sphere are given below:

$$x^2 + y^2 = r_i^2 \tag{21}$$

$$(x-a)^2 + (y-b)^2 + (z-c)^2 = L_i^2 \tag{22}$$

where (x,y,z) is the solution we are trying to find. At first glance it appears that this set of equations is underconstrained, with three unknowns and only two equations. However, in the scenario of Figure 8, $z = 0$ is guaranteed to be the solution in the local coordinate frame, hence we have two nonlinear equations in the two unknowns (x,y).

Expanding the sphere equation (22) with $z = 0$ and substituting the polar coordinates

$$\begin{aligned} x &= r\sin\theta \\ y &= -r\cos\theta \end{aligned} \tag{23}$$

in (21) and (22) yields the following equation:

$$A\cos\theta + B\sin\theta + C = 0 \tag{24}$$

where:

$$A = 2r_i b_i \qquad B = -2r_i a_i \qquad C = a_i^2 + b_i^2 + c_i^2 + r_i^2 - L_i^2$$

(24) has the same form as (14) and can be solved in the same way as shown earlier, by replacing E, F and G, with A, B and C, respectively. The solution is given by (16), (17) and (24) along with $z_{1,2} = 0$, which is the xyz solution in the local motor coordinate frame of Figure 8.

There are four possibilities regarding multiple solutions for each robot leg using the geometric approach:

1. The normal situation yields 2 possible valid solutions using equations (15-24).

2. When the discriminant in (15) is 0, there is only one solution since the circle is tangent to the sphere. This case represents the boundary of the useful orientational workspace and is a singularity.

3. When the discriminant in (15) is negative, the solution is imaginary, which means there are no solutions since the circle and sphere do not intersect. This case lies outside of the 3-SUR 1-RU orientational workspace.

4. There are infinite possible solutions when the circle lies on the surface of the sphere. For the 3-SUR 1-RU robot design, this case is always impossible by design.

6. 3-SUR 1-RU INVERSE ORIENTATION KINEMATICS EXAMPLES

This section presents two snapshot examples for the three-dof 3-SUR 1-RU parallel platform robot to demonstrate the analytical Inverse Orientation Kinematics Solution presented in this paper. Both examples use symmetric dimensions (length units are inches), i.e.:

$$\begin{aligned} R_1 &= R_2 = R_3 = R = 2.5 \\ L_1 &= L_2 = L_3 = L = 6 \\ L_A &= L_B = \frac{L}{2} = 3 \\ P_1 &= P_2 = P_3 = P = R = 2.5 \\ r_1 &= r_2 = r_3 = r = 1 \\ \delta_1 &= \varepsilon_1 = 330^\circ \\ \delta_2 &= \varepsilon_2 = 90^\circ \\ \delta_3 &= \varepsilon_3 = 210^\circ \end{aligned}$$

For both Examples presented below, both the analytical and geometric/analytical solution approaches yielded identical answers for the three servomotor angles $\{\boldsymbol{\Theta}\} = \{\theta_1 \quad \theta_2 \quad \theta_3\}^T$, both for elbow up and elbow down configurations.

Example 1. Nominal horizontal platform orientation

Given desired Euler angles $\alpha = 0$, $\beta = 0$, $\gamma = 0$, the following two solution sets are calculated:

a. servomotor angles $\{\boldsymbol{\Theta}\} = \{0^\circ \quad 0^\circ \quad 0^\circ\}$

elbow up

b. servomotor angles $\{\boldsymbol{\Theta}\} = \{161.1^\circ \quad 161.1^\circ \quad 161.1^\circ\}$

elbow down

Solution a (elbow up) for Example 1 is roughly pictured in the MATLAB graphic of Figure 9a and solution b (elbow down) is in Figure 9b.

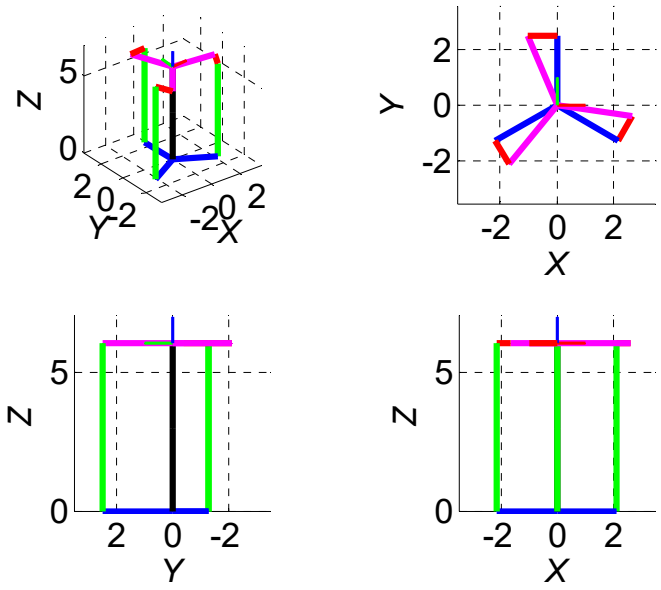

Figure 9a. Nominal Orientation Example 1 Solution a Elbow Up

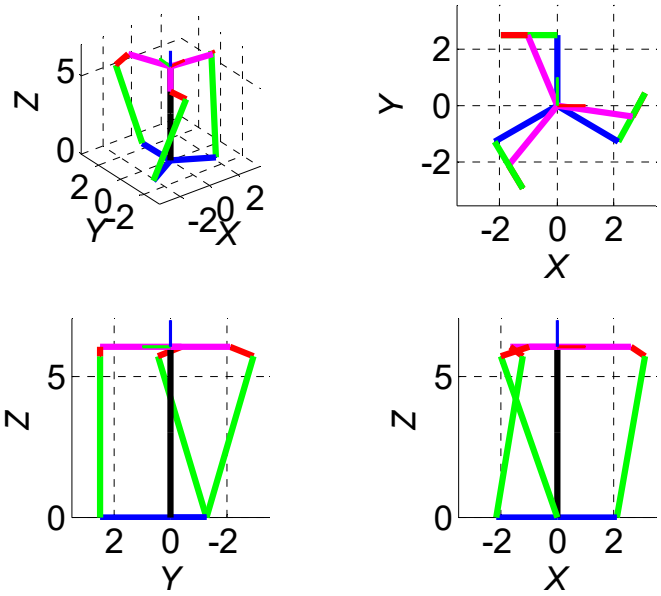

Figure 9b. Nominal Orientation Example 1 Solution b Elbow Down

Example 2. General platform orientation

Given desired Euler angles $\alpha = 4^\circ$, $\beta = 6^\circ$, $\gamma = 8^\circ$, the following two solution sets are calculated:

a. servomotor angles $\{\boldsymbol{\Theta}\} = \{-25.0^\circ \quad 18.9^\circ \quad 2.6^\circ\}$

elbow up

b. servomotor angles $\{\boldsymbol{\Theta}\} = \{177.7^\circ \quad 134.4^\circ \quad 165.4^\circ\}$

elbow down

Solution a (elbow up) for Example 1 is roughly pictured in the MATLAB graphic of Figure 10a and solution b (elbow down) is in Figure 10b. Solution set a. is **<u>invalid</u>** due to servo actuator joint limits (θ_i is negative, thus outside the allowable motor joint range $0^\circ \le \theta_i \le 180^\circ$).

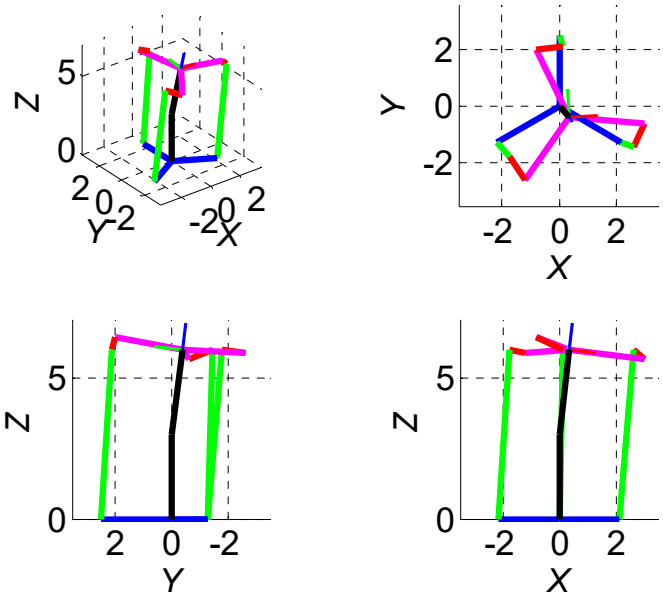

Figure 10a. Nominal Orientation Example 2 Solution a Elbow Up

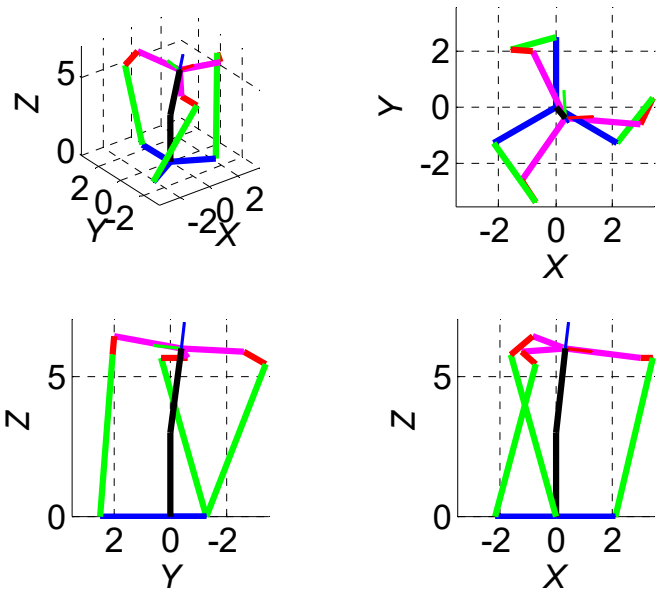

Figure 10b. Nominal Orientation Example 2 Solution b Elbow Down

7. CONCLUSION

This paper has presented a three-dof 3-SUR 1-RU parallel platform manipulator, designed to actively orient a UAV in yaw, pitch, roll, extended from a truss on the ground-based Windmobile driving on a runway. This robot is similar to classical 3-dof spherical parallel robots [6], with a new actuation scheme, design, application, and analytical inverse kinematics solution. The purpose is to test UAVs without requiring a wind tunnel. The 3-SUR 1-RU robot has three identical SUR legs in parallel, with the servomotor attached to the moving platform providing the R actuation in each case. There is also a passive fourth leg in the middle with an RU joint for support.

We presented two alternate methods to solve the inverse orientation kinematics (IOK) problem for the 3-SUR 1-RU parallel platform robot, which forms the basis for the control of the designed system. In both methods, each SUR leg is solved independently of the other two legs for its one rotary joint unknown angle. Then the same solution is applied independently to the other two legs.

The first method is the analytical solution. The analytical solution requires finding the roots of a quadratic polynomial for each leg (yielding elbow-up and elbow-down solutions). The alternative method is a geometrical/analytical solution based on finding the intersection point of a known circle and a known sphere; it also yields elbow-up and elbow-down solutions in general. The analytical solution is suitable for real-time implementation; the geometrical method is appealing due to the physical insight into the IOK problem.

If the requested Euler angles orientation cannot be achieved by the robot (i.e. they are outside of the orientational workspace) then both solutions for each will be imaginary and there is no possible solution in that case. Other potential solutions may be invalid due to violating input joint angle limits. Examples were presented to demonstrate the new platform robot IOK algorithm.

Future work plans for the 3-SUR 1-RU robot in the Windmobile Project include solution of Forward Orientation Kinematics, completion of the robot construction, controller design and implementation, and experimental data collection, both for the platform robot itself and in service taking aerodynamic data for the Galah UAV.

ACKNOWLEDGEMENTS

We would like to thank Joey Feck, Ohio University graduate research assistant, for the CAD drawings.

REFERENCES

[1] Zeng, D., Zhen, H., & Lu, W. (2008). Performance analysis and optimal design of a 3-dof 3-PRUR parallel mechanism. *Journal of Mechanical Design*, *130*(042307), 1-9.

[2] Mangan, B. (2010). Application of robotic technology in biomechanics to study joint laxity. *Journal of Medical Engineering and Technology*. 34(7) 399-407.

[3] Liu, G., Lou, Y., & Li, Z. (2003). Singularities of parallel manipulators: A geometric treatment. *IEEE Transactions on Robotics and Automation*, *19*(4), 579-594.

[4] Di Gregorio, R. (2003). Kinematics of the 3-upu wrist. *Mechanism and Machine Theory*, *38*, 253-263.

[5] Deidda, R., Mariani, A., & Ruggiu, M. (2010). On the kinematics of the 3-RRUR spherical parallel manipulator. *Robotica*, *28*, 821-832.

[6] http://www-sop.inria.fr/members/Jean-Pierre.Merlet/Archi /node8.html

[7] Craig, J.J., 2005, Introduction to Robotics: Mechanics and Control, Addison Wesley Publishing Co., Reading, MA.